Assessing the high frequency behavior of non-polarizable electrodes for spectral induced polarization measurements

Feras Abdulsamad, Nicolas Florsch, Myriam Schmutz, Christian Camerlynck

Journal of Applied Geophysics

Assessing the high frequency behavior of non-polarizable electrodes for spectral induced polarization measurements

Feras Abdulsamad[1,*], Nicolas Florsch[1,2], Myriam Schmutz[3], Christian Camerlynck[1]

[1] *Sorbonne Université, UPMC Univ Paris 06, CNRS, EPHE, UMR 7619 Metis, 4 place Jussieu, 75005 Paris, France*

[2] *Sorbonne Université, UPMC Univ Paris 06, UMI 209 Ummisco, 4 place Jussieu, 75005 Paris, France*

[3] *Bordeaux-INP, ENSEGID, EA4592, 1 allée Daguin, 33607 Pessac, France.*

[*] *Corresponding author*

Email address:

feras.abdulsamad@upmc.fr
nicolas.florsch@upmc.fr
myriam.schmutz@ensegid.fr
christian.camerlynck@upmc.fr

Abstract

During the last decades, the usage of spectral induced polarization (SIP) measurements in hydrogeology and detecting environmental problems has been extensively increased. However, the physical mechanisms which are responsible for the induced polarization response over the usual frequency range (typically 1 mHz to 10-20 kHz) require better understanding. The phase shift observed at high frequencies is sometimes attributed to the so-called Maxwell-Wagner polarization which takes place when charges cross an interface. However, SIP measurements of tap water show a phase shift at frequencies higher than 1 kHz, where no Maxwell-Wagner polarization may occur. In this paper, we enlighten the possible origin of this phase shift and deduce its likely relationship with the types of the measuring electrodes. SIP Laboratory measurements of tap water using different types of measuring electrodes (polarizable and non-polarizable electrodes) are carried out to detect the origin of the phase shift at high frequencies and the influence of the measuring electrodes types on the observed complex resistivity. Sodium chloride is used to change the conductivity of the medium in order to quantify the solution conductivity role. The results of these measurements are clearly showing the impact of the measuring electrodes type on the measured phase spectrum while the influence on the amplitude spectrum is negligible. The phenomenon appearing on the phase spectrum at high frequency (>1 kHz) whatever the electrode type is, the phase shows an increase compared to the theoretical response, and the discrepancy (at least in absolute value) increases with frequency, but it is less severe when medium conductivity is larger. Additionally, the frequency corner is shifted upward in frequency. The dependence of this phenomenon on the conductivity and the measuring electrodes type (electrode-electrolyte interface) seems to be due to some dielectric effects (as an electrical double layer of small relaxation time formed at the

electrodes interface). Therefore, this dielectric response should be taken into account at high frequency to better analytically separate the medium own response from that linked to the measuring electrodes used. We modelled this effect by adding a capacitance connected in parallel with the traditional equivalent electric circuit used to describe the dielectric response of medium.

Keywords: spectral induced polarization, phase shift, high frequency effects, non-polarizable electrodes, measuring electrodes.

1. Introduction

While the induced polarization method is still widely used in mineral exploration (e.g. Pelton et al. 1978; Luo and Zhang, 1998), it is today currently used for engineering and environmental studies, mapping of polluted area and for detecting organic contaminated zones (Vanhala et al., 1992; Slater and Lesmes, 2002; Gazoty et al., 2012). In addition, it is used in hydro-geophysical application to calculate the hydraulic conductivity of subsurface formation (Binley et al., 2005; Hördt et al., 2007; Revil and Florsch, 2010). In parallel, the complex impedance is used in biomedical engineering in similar frequency ranges (Schwan, 1968; Ragheb and Geddes, 1991).

So far, the physical mechanisms responsible for the induced polarization over the frequency range are not completely identified. Numerous mechanisms are able to generate the observed effects. The most involved mechanisms are (i) electrochemical polarization that corresponds to reversible electrochemical and diffusion processes (Zonge, 1972 ; Luo and Zhang, 1998) which take place at low frequency, and (ii) interfacial polarization mechanisms, which is also called Maxwell-Wagner polarization (Vinegar and Waxman, 1984; Lesmes and Morgan, 2001; Tabbagh et al., 2009) take place at higher frequencies (generally over 1 kHz). Among the models used to study these mechanisms, electrical circuit analog which consists of resistors and capacitances are found useful. In this frame, each element of the circuit represents a physical phenomenon. The electric double layer may be simulated by the association of one capacitance C_{dl} with a resistance r_{ct} (charge transfer resistance across the electric double layer), whereas the diffusion effects at low frequency caused by the electrochemical polarization mechanism in the presence of metal-electrolyte interface could be presented by a Warburg impedance Z_w (Merriam, 2007).

Furthermore, the problem of using noble measuring electrodes, which do not affect the measured electrical potential, goes back to the early days of using the geoelectrical method in

geophysical prospecting (Schwan, 1968). The effects of the measuring electrodes type on the apparent resistivity and the apparent chargeability measured in time domain induced polarization measurements were studied and proved by LaBrecque and Daily (2008). From their measurements using direct current on tap water only, and on sand saturated with tap water, they found that, the errors in chargeability and in resistivity depend on the electrode type, and the measurements discrepancies depend on the electrode chemical properties. The discrepancies were lower in tap water case than the one with saturated sand. Furthermore, the influence of the type of measuring electrodes on chargeability is higher than on resistivity, and that is expected due to the weaker measured signal in chargeability measurements when signal to noise ratio is low.

On the other hand, spectral induced polarization (SIP) was extensively developed in laboratory, thanks to the possibility of carrying out measurements in a wide-frequency range without signal pollution caused by electromagnetic coupling. In order to acquire high quality data, both measurement devices and sensors (electrodes) have to be well suited (Vanhala and Soininen, 1995). Measurement devices, such as SIP Fuchs (Radic Research Ltd) or SIP Zel (Zimmermann et al., 2008) are adapted for both field and laboratory experiments with high accuracy, but the electrode issue is still important and needs more developments to find the optimal electrode which has a minimum impact on the measured potential.

The electrode issue concerns more environmental and hydro-geophysics purposes where the measured phase is small ($\leq$ 10 mrad) (Zimmermann et al., 2008) as noticed in many studies (e.g., Slater and Lesmes, 2002; Schmutz et al., 2010).

The influence of both distance between the measuring electrodes and their inclination on the SIP measurements was studied by Vanhala and Soininen (1995). They found that the small distance (smaller than 5 cm) between electrodes could produce noise in the phase spectrum, furthermore, the tilt effect of non-vertical measuring electrodes decreases with

increasing distance between them. The influence of the active geometry (surface of electrode-medium interface) of the measuring electrodes on the complex resistivity measured was studied by Riaz and Reifsnider (2010). They found that at high frequency the complex resistivity is not as dependent on active geometry as at low frequency.

In fact, our work here was focused on the dielectric effect that appears on the phase spectrum at high frequencies, and on its dependence with the type of measuring electrodes. The phase shift observed at high frequency is usually attributed to polarization mechanism which is called Maxwell-Wagner polarization (occurring when charges cross an interface). In water, the phase shift observed at high frequency is generally higher than that arises from the dielectric permittivity of water. The absence of Maxwell-Wagner polarization and coupling effects, leads us to think that another dielectric phenomenon occurs at the electrode-electrolyte interface (absorption, diffusion or/and electrical double layer). So in the first part we interpreted the high frequency effect as a dielectric phenomenon and in the second part we encapsulated this effect in an electronical equivalent circuit.

Therefore, series of SIP measurements using tap water were carried out by using different conventional types of measuring electrodes (polarizable and non-polarizable). Each electrode has its own advantage and disadvantage regarding the accuracy and the usability in the laboratory or in the field.

As many other studies which aimed to test electrodes stability (Vanhala and Soininen, 1995) or to test the accuracy of SIP instruments (Zimmermann et al., 2008), we used tap water as a medium in our study: the theoretical spectral induced polarization response of water could be calculated using the approximate value of the water relative dielectric permittivity of ($\varepsilon_r = 80$) and the water measured conductivity.

2. Experimental setup

Complex resistivity measurements were carried out over the frequency range from 0.183 Hz to 20000 Hz using the SIP Fuchs III equipment developed by Radic Research (see http://www.radic-research.homepage.t-online.de/).

The measurements have been performed by using tap water with different salinity concentrations. Sodium chloride was used to change the conductivity and consequently the ions concentration in the medium. A plastic box with dimensions of 50 x 33 x 23 cm (LxWxH) was used as a sample holder, filled with 22 cm of water. Wenner configuration was used with electrode spacing of 10 cm. The small distance between electrodes could affect the phase spectrum (Vanhala and Soininen, 1995). The current electrodes are made of stainless steel (Ag 316L) electrodes fixed at the extremity of the device (30 cm apart). A low current was used to ensure linearity and to avoid too large current density in the medium. To check for repeatability, the SIP measurements were repeated five times over the mentioned frequency range; later the standard deviation was calculated at each frequency and presented as error on each frequency...

Temperature, pH and conductivity of the medium were measured in parallel. The pH of the medium varies between 7.62 and 7.92 depending on the salinity level. The temperature of the medium varies between 16.2 °C and 16.6 °C during the experiment. As the variation of the temperature is very small, no thermal correction has been applied on the complex resistivity measurements.

The conductivity of the water was measured directly by using a conductivity-meter (a WTW LF 340) which allows to calculate the water theoretical response, and to set the geometric factor taking into account the position of the electrodes and the boundary conditions. In this way, the apparent real and imaginary measured amplitudes are correctly calibrated, while the apparent phase is independent of the geometric factor.

Before starting the SIP measurements, a test of both the instrument accuracy and calibration was performed by using electric circuit of known response (Vanhala and Soininen, 1995; Titov et al., 2010). The circuit components (resistors and capacitances) and their installation were chosen to give weak phase response (a few mrad) at high frequencies. The relative theoretical response is supposed to be close to that measured in tap water by different kinds of electrodes. Figure 1 shows the measured phase and amplitude, and the theoretical electric circuit spectral response. The result shows the high accuracy of the instrument over the entire frequency range with error less than 0.1 mrad at low frequency (< 10 Hz) and less than 0.5 mrad at high frequency. This high accuracy used in our experiments excludes any impact of the instrument on the measured response.

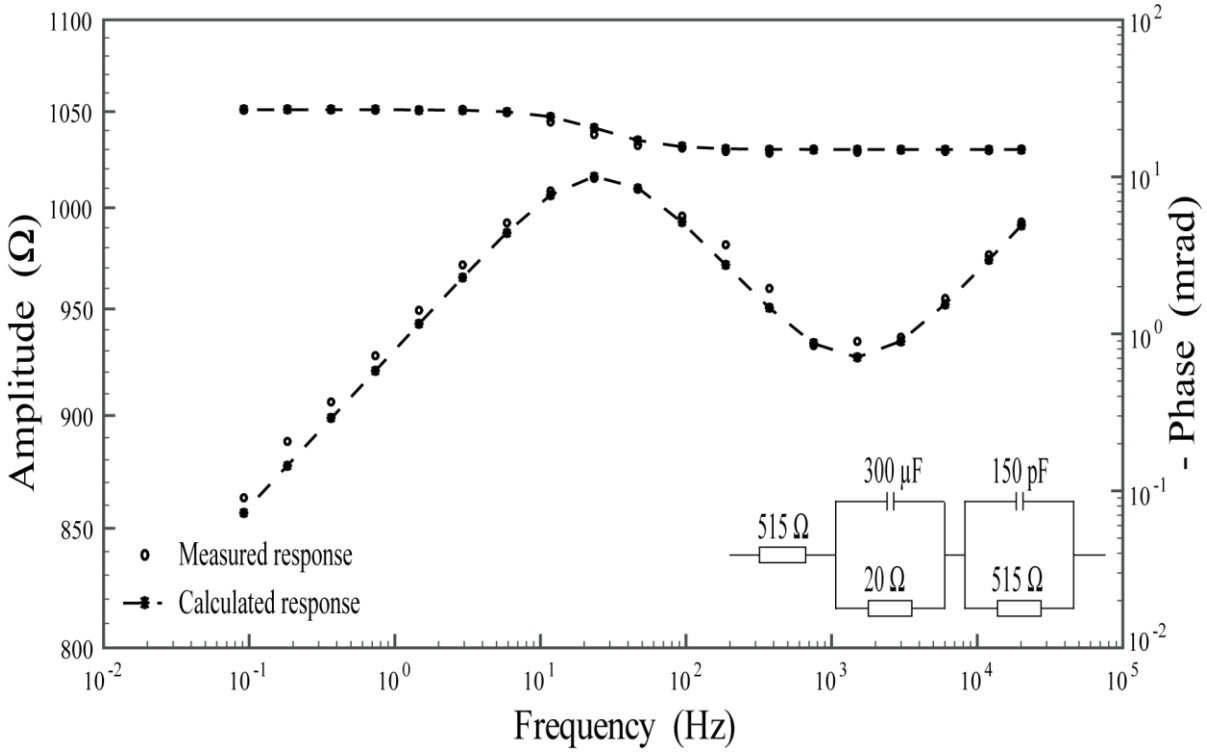

Fig. 1: instrument accuracy test with the electric circuit used.

3. Electrodes preparation

171 To characterize the impact of the measuring electrodes on the high frequency phase
172 shift, we tested various conventional electrodes (figure 2) usually used in SIP. Polarizable
173 316L stainless steel metal electrodes and three non-polarizable electrodes (Ag/AgCl filled
174 with saturated KCl solution; Ag/AgCl filled with a mixed of KCl-agar gel; $Cu/CuSO_4$
175 electrodes) are used in this study. The non-polarizable electrodes are hand-made and prepared
176 in our laboratory.

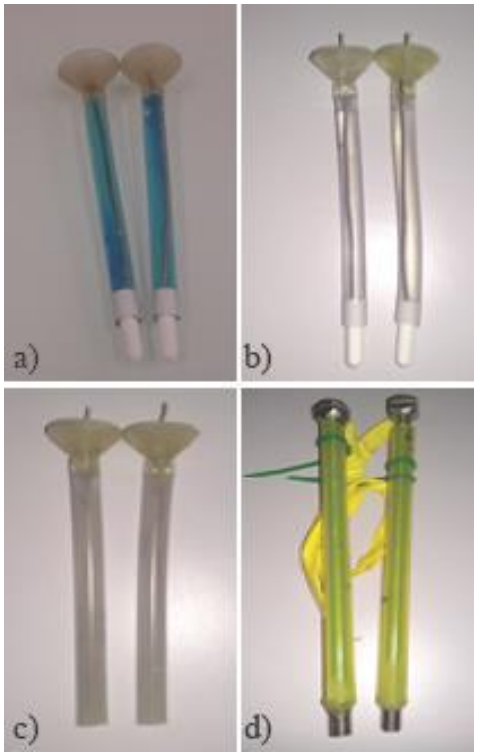

177

178 Fig. 2: the electrodes used in our study, a) $Cu/CuSO_4$ electrodes; b) Ag/AgCl-KCl
179 electrodes; c) Ag/AgCl-Agar-gel electrodes; d) 316L Stainless steel electrodes (with yellow
180 plastic coating).
181

182 Ag/AgCl and $Cu/CuSO_4$ electrodes have the same conceptual schema which is presented
183 in figure 3. They consists in a metal wire immerged in oversaturated electrolyte of the metal
184 and a permeable ceramic between the medium and the electrode. One can notice that even
185 with low permeable ceramics, a little electrolyte is released into the medium, which may
186 affect the SIP measurements over time. We operate as quickly as possible to minimize this

risk. The preparation of the Ag/AgCl starts by bleaching the silver wire during few hours and then the silver wire is connected to a 6 Volt battery and placed in KCl solution during ten minutes (electroplating gives the electrode more stability with time). After that, the wire is soaked in a saturated KCl solution. The use of agar gel to prepare non-polarizable electrodes is common to overcome the leakage problem during long duration experiments. Precipitation of Agar powder is forced by using a 1 mol/l KCl solution. The agar gel is a good conductor without any polarization effects, and its use has already been described for polarization studies (Scott, 2006; Hördt and Milde, 2012). Solidified Agar gel avoids the use of porous ceramic.

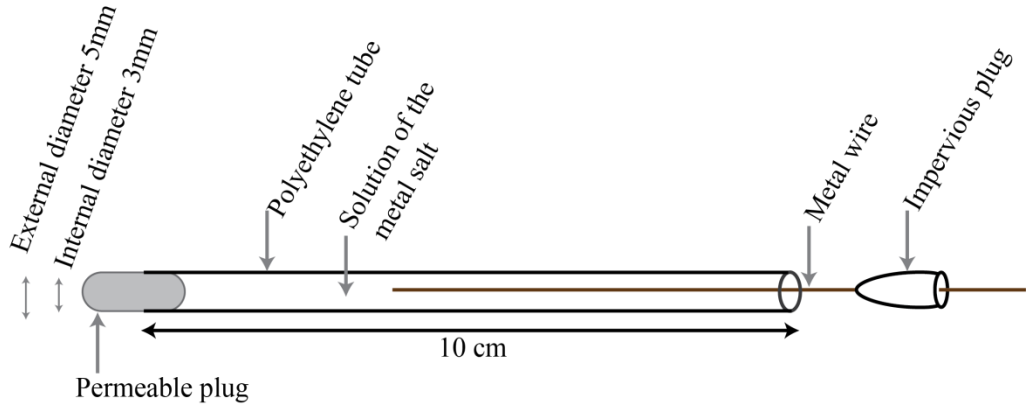

Fig. 3: outline of the non-polarizable electrode

Since the electrodes pairs are built up following the same process, the DC potential difference between them will be very close to zero. For this reason, we may consider that they are non-polarizable (or more objectively, a constant weak differential polarization within each pair). In such a configuration, the measured data should not be affected by the presence of measuring electrodes and then the response should not depend on the electrode.

After preparing the non-polarizable electrodes, all (metal and non-polarizable) were placed in a water tank to measure the self-potential of each electrode type during 2 hours, using a recording digital multimeter (Keithley 2701 Multimeter). Figure 4 (left) shows

example of self-potential values measured in the electrodes used in this study. Later the potential difference between each pair of electrodes was calculated and presented in figure 4 (right). This electrode monitoring shows that non-polarizable electrodes have more stability with time and lower self-potential values than the stainless steel electrodes (usually used in filed measurements) in correlation with the results of Vanhala and Soininen (1995) and Dahlin et al. (2002). The Ag/AgCl electrodes show the lowest self-potential and the best stability over time, with potential difference between electrodes less than 1 mV. The $Cu/CuSO_4$ electrodes have the same trend of stability over time and the potential difference is around 1 mV, but we notice also that there are some more or less 40 min transients, may be due to electrode leakage. The Ag/AgCl filled with KCl-agar gel electrodes show high variations over the time at the beginning (2 hours after preparation) before reaching electrical stability and a potential difference close to 1 mV at least 3 hours after their preparation. It is therefore recommended to use these electrodes only a few hours after preparation. The stainless steel electrodes have the highest charge-up and no stability over the time, where the potential difference for the electrodes pair increases with time up to 12 mV at the end of monitoring.

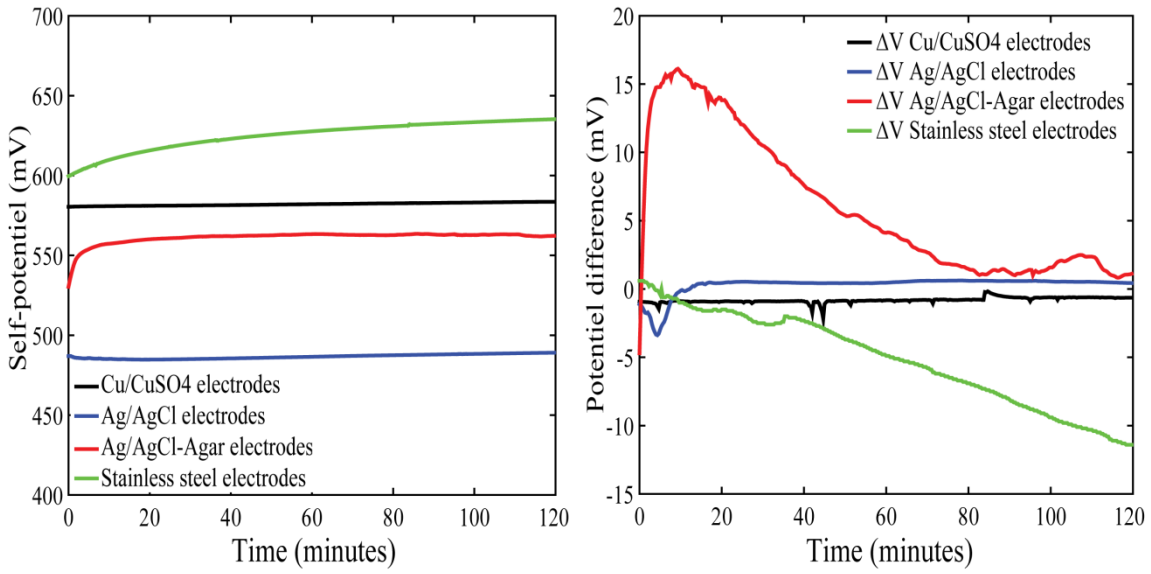

Fig. 4: left) electrode self-potential. Reference electrode is a NaCl-type $Pb\text{-}PbCl_2$ electrode (Petiau, 2000); right) potential difference for each electrode pair type. Origin time corresponds to 1 hour after electrode preparation.

4. Results and discussion

The complex resistivity measurements of tap water show a phase shift at high frequency for all the measuring electrodes types. In order to assess the own phase shift we compare the results of our measurements with the theoretical water spectral induced polarization response. The theoretical dielectric response of the medium could be calculated by using the following equations 1 and 2:

$$\sigma(\omega) = \sigma_0 + \mathrm{j}\ \omega\ \varepsilon_0\ \varepsilon_r \quad (1)$$

$$\rho(\omega) = 1/\sigma(\omega) \quad (2)$$

where $\sigma(\omega)$ and $\rho(\omega)$ are respectively the complex conductivity and the complex resistivity, σ_0 is the DC conductivity, j is the imaginary unit, ε_r is the relative dielectric permittivity, and ε_0 is the free space permittivity and its value is 8.854 10^{-12} F/m. By using the water conductivity measured with the conductivity-meter and using the approximate value of the relative dielectric permittivity of fresh water $\varepsilon_r = 80$, we get the theoretical response of water over the frequency range of our measurements (Vanhala and Soininen, 1995; Zimmermann et al, 2008). The measured instrumental phase $\varphi(\omega)$ is defined as the ratio between real and imaginary components of the complex resistivity, whereas the theoretical phase could be calculated from equation 3:

$$\varphi(\omega) = -\omega\ \varepsilon_0\ \varepsilon_r\ /\sigma_0 = -\omega\ \rho_0 \varepsilon_0\ \varepsilon_r \quad (3)$$

where $\rho_0 = 1/\sigma_0$ is the DC resistivity.

Figure 5 shows the amplitude and phase spectra of the complex resistivity (corresponding to 18 Ωm water resistivity) obtained by using the four different pairs of electrodes mentioned above. All measured amplitudes are close to the expected response with

a satisfying repeatability, whereas the phase measured showed more variation over the frequency range especially at high frequencies.

The phase measured by non-polarizable electrodes shows very small variation over the low frequency range (0.183 Hz to 1 kHz), while the one that is measured by stainless steel electrodes over the same frequency range shows larger variation. However, this result was expected because of the instability behavior of these electrodes showed by the self-potential difference record. It is therefore recommended to use non-polarizable electrodes over the whole frequency range (figure 5).

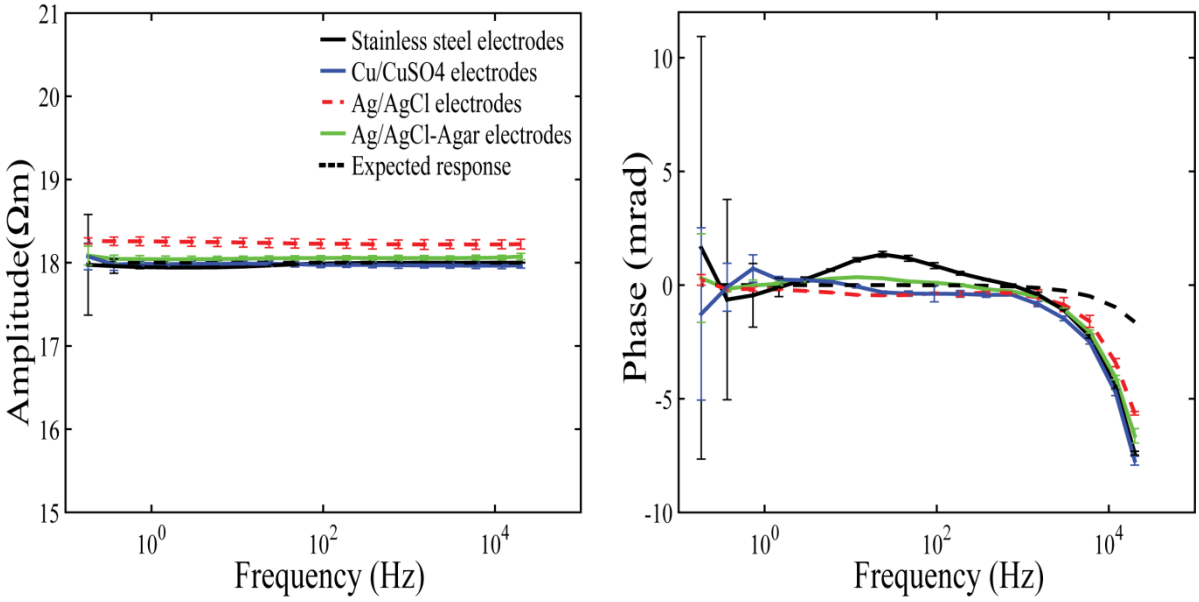

Fig. 5: amplitude (left) and phase (right) of the water complex resistivity by using four types of electrodes.

However, the phases at high frequencies (> 1 kHz) are larger than expected for the four electrode types. For instance, the phase relative to the Ag/AgCl electrodes is found three times larger than the theoretical phase within the high frequency range (> 1 kHz). Hence, these measurements should be linked to a relative dielectric permittivity 3 times larger than the water relative dielectric permittivity.

By comparing the phase measured over the last frequency decade (1 kHz – 20 kHz) with metal and $Cu/CuSO_4$ electrodes, we notice that the respective phases are very close despite the difference in electrode nature. Through the contact resistance of the stainless steel electrodes might be notably lower than the one of the porous ceramic $Cu/CuSO_4$ electrodes; it is likely that the contact quality is not a major causing the high frequency trend.

Figure 6 illustrates the phase measured at three salt concentrations (corresponding to 18, 10 and 5 Ωm water resistivity) when using Ag/AgCl electrodes and $Cu/CuSO_4$ respectively. One observes a dependence of the high frequency response on water conductivity, and phase responses shift toward high frequency when water conductivity increases. When changing the medium conductivity by adding a little NaCl to remain within the given indicated range (water resistivity between 5 and 18 Ωm, meaning water electrical conductivity less than 200 mS/m; for instance, see fig. 1 from (Bouksila et al., 2008)), the relative dielectric permittivity remains unchanged, close to 80. While the measured phase shift is 3 to 5 times higher than the expected theoretical phase shift, a change in water dielectric permittivity cannot be invoked as an explanation.

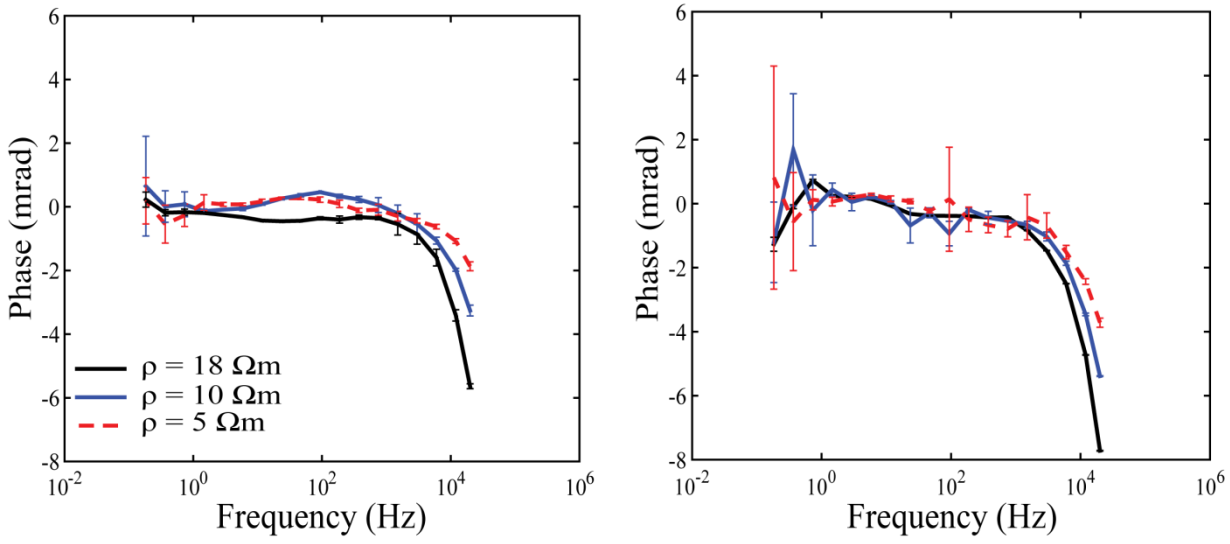

Fig. 6: apparent phase measurements for the 3 salinity levels: left) Ag/AgCl electrodes; right) Cu/CuSO4 electrodes.

Figure 7 shows the phase difference between the measured phase and the theoretical one calculated from equation (3) at the highest frequency (20 kHz) where the difference is higher. In all cases the theoretical responses were calculated with the same relative dielectric permittivity ($\varepsilon_r = 80$) and by changing the solution conductivity in the equation (3).

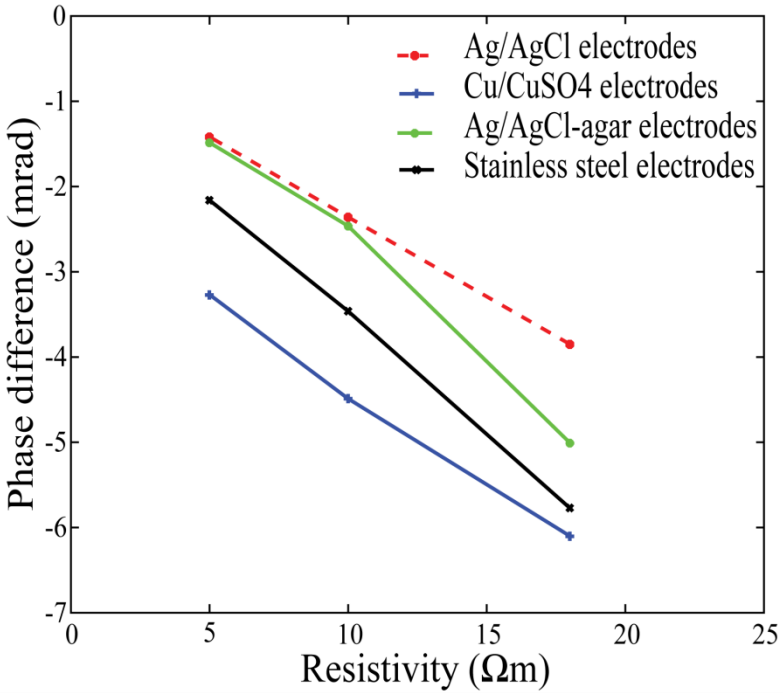

Fig 7: phase difference between measured and expected data as function of the solution resistivity at frequency 20 kHz.

Since no coupling effects are disturbing the measurements thanks to the laboratory box scale, (e.g. Ghorbani et al., 2009) and after checking with an accuracy test (figure1), these observations from figures 6 and 7 could only be explained by the change of the electrochemical conditions at the electrode-electrolyte interface, where the ions concentration around the measuring electrodes had increased after adding NaCl in the medium. That means that the electrochemical changes in the electrode vicinity impact the measure. Adsorption or diffusion of ions near the porous ceramic and/or the electrical double layer existing at the electrode-electrolyte interface are responsible for the additional effects measured at high frequency, that we call “dielectric” but just because it looks like dielectrical.

Finally, the possible influence of the current density on high frequency effect was also studied, by using double and half of the initial current density (360 mA) used in our measurements. There is no remarkable influence on the phase measured when the current density varies between 180 mA to 720 mA.

5. Empirical modelling

The response of a traditional medium, as a soil sample, can be represented by one of the many empirical dielectric models (e.g. Debye model, Cole-Cole model or Cole-Davidson model). They are traditionally depicted by an equivalent electronic circuit (Marshall et Madden, 1959; Dias, 1972; 2000). The simplest equivalent circuit contains two parallel electric paths: the first path consists of a simple resistor and represents the pure ohmic conduction associated to a free ionic path (current path at low frequency or direct current), whereas the second path contains several electronic components (resistors and capacitances) which model the polarization effects of the medium associated with the metal or clay grains in contact with the pore electrolyte. The latter part of the circuit models the response of the medium in the SIP frequencies. Dias (2000) provides such a collection of equivalent circuits. One classical microscopic polarizable model and its circuit is shown on figure 8 (Dias, 1972; 2000).

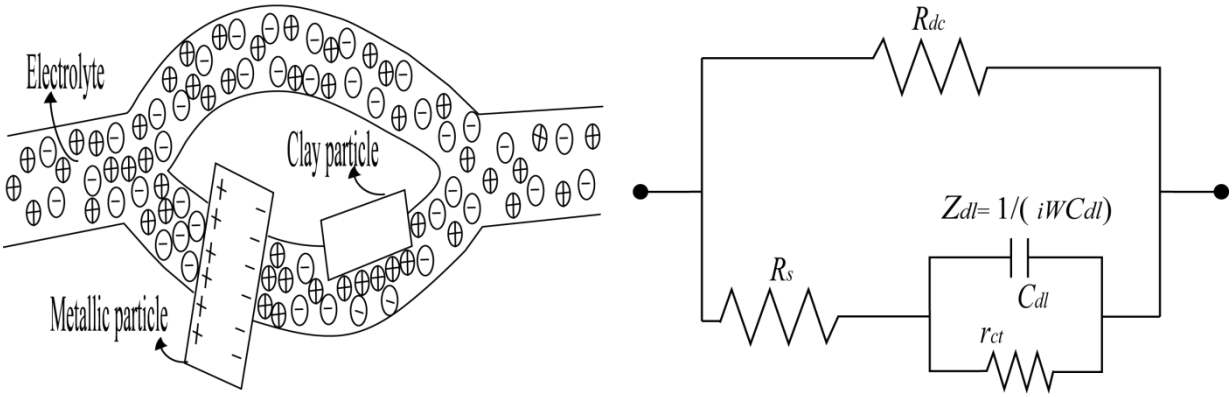

Fig. 8: the electric paths in polarizable medium (left) and equivalent electrical circuit for a polarizable medium (right), (modified from (Dias, 2000)). Here C_{dl} is the electric double layer capacitance, Z_{dl} the complex impedance of the electric double layer, r_{ct} the charge transfer resistance, R_s is the resistivity of the electrolyte filling the material and R_{dc} is the sample resistivity in direct current.

From the measurements of this study and other data sets (e.g. Joseph et al., 2015), we notice the correlation between the effects at high frequency and medium resistivity. As long as the medium resistivity increases, the high frequency effect appears earlier on the frequency range (shifted to low frequency) and its amplitude becomes significant. Therefore, a model including the high frequency dielectric phenomena formed at the electrode-electrolyte interface (clearly linked to the measuring electrodes type) in the equivalent electric circuit should be sensitive to the total electric response of the medium, since the electric response is related to the electrical and electrochemical properties of the medium. Figure 9 presents the equivalent circuit we propose to accommodate the "high frequency dielectric phenomenon", where it is modeled by a capacitance C_{hf} connected in parallel with the equivalent circuit of the medium response. The magnitude of this capacitance is small in order of nanoFarads. This model is a general model to fit SIP measurements from medium contains different phases (solid and liquid).

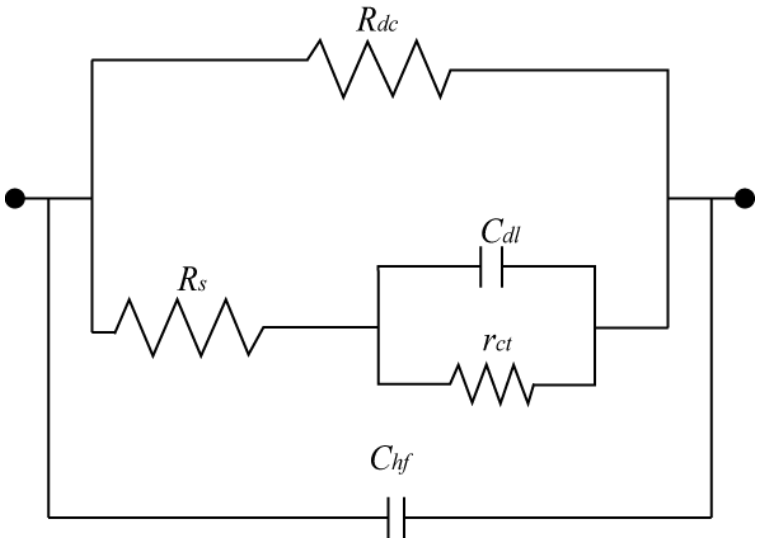

Fig. 9: the equivalent electric circuit models the high frequency dielectric phenomenon where C_{hf} is a low value capacitance.

Finally, in order to fit our data measured which are a special case of SIP measurements (the medium is a one phase medium), a simple circuit consists of resistance (R_{dc}) connected on parallel with a capacitance C_ε (($C_\varepsilon = \varepsilon_r * \varepsilon_0$) which represents the dielectric response of the medium), could present the medium theoretical response. Figure 10 shows the amplitude and phase fitting the Ag/AgCl electrodes in water with resistivity 18.2 Ωm. At frequencies greater than 1 kHz, measured and modeled (from electric analog) phase curves are superimposed. At lower frequencies, the fit is not so accurate with a small discrepancy of 0.3 mrad, which may be linked to the filter 60 Hz (does not work well), but this frequency range is not targeted in study.

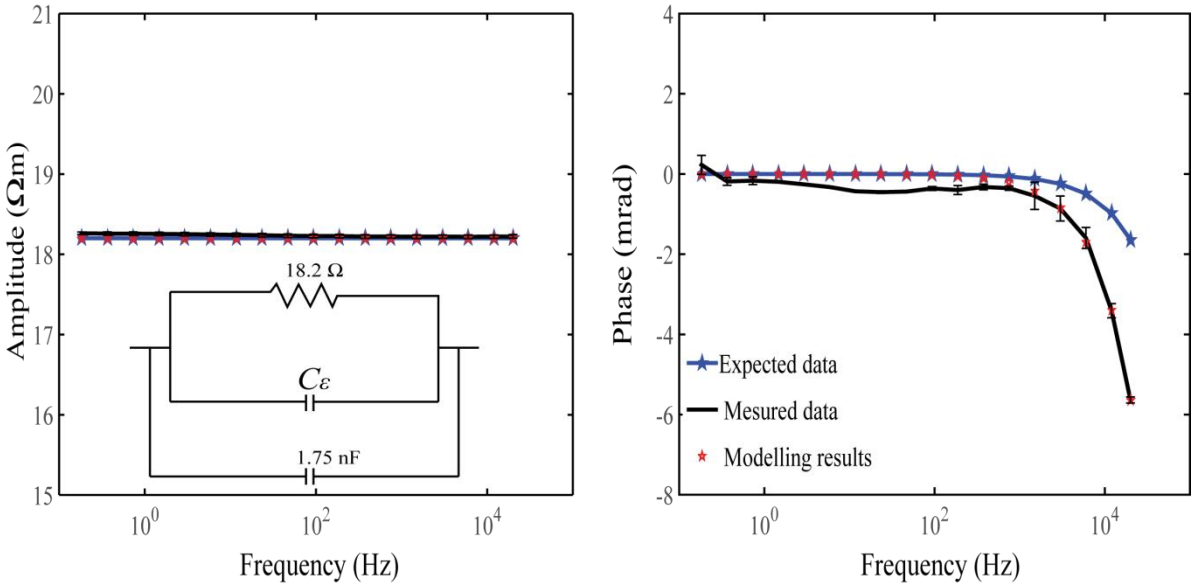

Fig. 10: modelling the measurements with Ag/AgCl electrodes. Water DC Resistivity is 18.2 Ω m. Left) the equivalent electric circuit with adjusted values is shown and amplitude spectrum; right) phase spectrum.

6. Discussion and conclusion

Once the instrument accuracy is checked and the stability with time of a set of 4 various built up electrodes verified, we observe a dependence of the response of the whole on the measuring electrode nature. The differences emerge in the high frequency part of the spectrum, saying above 1 kHz. It is the range where the IP response origin is neither consensual nor really understood yet. Actually, the "normal" permittivity of water, playing the role of the medium, impact this high frequency (> 1 kHz) domain as well, but is typically 3 or 4 times smaller than the actual observed response. We get satisfactory data fits by assuming a superimposition of the response relative to the electric permittivity of the medium plus a contribution of the electrode which depends on the electrode nature. We can presume that the electrode/electrolyte double layer is responsible for that contribution, for which the theory must still be done. As a matter of fact, a capacitance just set in parallel with the measuring electrodes permits to fit the observation in a very satisfactory manner. It is equivalent to introduce the same electronic (fitting device) in parallel with the medium, but this approach is

only opportunistic since we are supposed to measure only the medium response and not the electrodes which have only the role of sampling the potential within the medium.

As far as the SIP or TDIP are concerned, it is useful to split the high frequency response into these two contributions: one representative of the medium (and it generally assumes a relative permittivity of reasonable value), and the other relative to the electrode pair. This double contribution permits finally to take into account, -to accommodate for- the measuring electrode specific response when processing IP data, especially when processing high quality data at the lab scale as well as on the field, to finally correctly assess the chargeability, time constant of any and other IP parameters describing the investigated medium.

Acknowledgement:

We wish to thank particularly Dr. A. Maineult for his very helpful availability, especially during the experimental phase of this study. We also thank anonymous reviewers for their helpful suggestions.

References

Binley, A., L. D. Slater, M. Fukes, and G. Cassiani. 2005. Relationship between spectral induced polarization and hydraulic properties of saturated and unsaturated Sandstone. *Water Resources Research*, 41(12): W12417. doi:10.1029/2005WR004202.

Bouksila, F., M. Persson, R. Berndtsson, and A. Bahri, 2008. Soil water content and salinity determination using different dielectric methods in saline gypsiferous soil. Hydrological Science Journal, 53(1): 253-265. doi:10.1623/hysj.53.1.253

Dahlin, T., V. Leroux, et J. Nissen, 2002. Measuring techniques in induced polarisation imaging. *Journal of Applied Geophysics*, 50(3): 279‑98. doi:10.1016/S0926-9851(02)00148-9.

Dias, C. A., 1972. Analytical model for a polarizable medium at radio and rower Frequencies. *Journal of Geophysical Research*, 77(26): 4945‑4956. doi:10.1029/JB077i026p04945.

Dias, C. A., 2000. Developments in a model to describe low-frequency electrical polarization of rocks. *Geophysics*, 65(2): 437‑51. doi:10.1190/1.1444738.

Gazoty, A., G. Fiandaca, J. Pedersen, E. Auken, and A.V. Christiansen, 2012. Mapping of landfills using time-domain spectral induced polarization data: the Eskelund case study. *Near Surface Geophysics*, 10(1957). doi:10.3997/1873-0604.2012046.

Ghorbani, A., Camerlynck, C., Florsch, N., 2009. CR1Dinv: A Matlab program to invert 1D spectral induced polarization data for the Cole–Cole model including electromagnetic effects, Computers & Geosciences, Volume 35, Issue 2, http://dx.doi.org/10.1016/j.cageo.2008.06.001.

Hördt, A., and S. Milde, 2012. Studies with gel-filled sandstone samples with implications for the origin of induced polarization. *Near Surface Geophysics*, 10(1957). doi:10.3997/1873-0604.2011041.

Hördt, A., R. Blaschek, A. Kemna, and N. Zisser, 2007. Hydraulic conductivity estimation from induced polarisation data at the field scale — the Krauthausen case history. *Journal of Applied Geophysics*, 62 (1):33‑46. doi:10.1016/j.jappgeo.2006.08.001.

Joseph, S., M. Ingham, and G. Gouws, 2015. Spectral induced polarization measurements on New Zealand sands - Dependence on fluid conductivity. *Near Surface Geophysics*, 13(2061). doi:10.3997/1873-0604.2014043.

LaBrecque, D., and W. Daily, 2008. Assessment of measurement errors for galvanic-resistivity electrodes of different composition ». *Geophysics*, 73(2):F55‑64. doi:10.1190/1.2823457.

Lesmes, D. P., and F. D. Morgan, 2001. Dielectric Spectroscopy of Sedimentary Rocks. *Journal of Geophysical Research: Solid Earth*, 106(B7):13329‑46. doi:10.1029/2000JB900402.

Luo, Y., and Zhang, G., 1998. Theory and application of spectral induced polarization. *Soc. Expl. Geophy.*, 32pp.

Marshall, D., and T. Madden, 1959. Induced polarization, a study of its causes. *Geophysics*, 24 (4): 790‑816. doi:10.1190/1.1438659.

Merriam, J, 2007. Induced polarization and surface electrochemistry. *Geophysics*, 72(4): F157‑66. doi:10.1190/1.2732554.

Pelton, W., S. Ward, P. Hallof, W. Sill, and P. Nelson. 1978. 'Mineral Discrimination and Removal of Inductive Coupling with Multifrequency Ip'. Geophysics 43 (3): 588–609. doi:10.1190/1.1440839.

Petiau, G., 2000. Second generation of leas-lead chloride electrodes for geophysical

438 applications, Pure and Applied Geophysics, 157(2000):357-382.
439 Ragheb, T., and L. A. Geddes, 1991. The Polarization Impedance of Common Electrode
440 Metals Operated at Low Current Density. *Annals of Biomedical Engineering*, 19(2):
441 151‐63.
442 Revil, A., and N. Florsch, 2010. Determination of permeability from spectral induced
443 polarization in granular media. *Geophysical Journal International*, 181(3):1480‐98.
444 doi:10.1111/j.1365-246X.2010.04573.x.
445 Riaz, A., and K. Reifsnider, 2010. Study of influence of electrode geometry on impedance
446 spectroscopy , 167‐75. doi:10.1115/FuelCell2010-33209.
447 Schmutz, M., A. Revil, P. Vaudelet, M. Batzle, P. Femenía Viñao, and D. D. Werkema, 2010.
448 Influence of Oil Saturation upon Spectral Induced Polarization of Oil-Bearing Sands.
449 *Geophysical Journal International*, 183(1):211‐24. doi:10.1111/j.1365-
450 246X.2010.04751.x.
451 Schwan, H. P., 1968. Electrode polarization impedance and measurements in biological
452 materials. *Annals of the New York Academy of Sciences*, 148(1):191‐209.
453 doi:10.1111/j.1749-6632.1968.tb20349.x.
454 Scott, J., 2006. The origin of the observed low-frequency electrical polarization in sandstones.
455 *Geophysics*, 71(5):G235‐38. doi:10.1190/1.2258092.
456 Slater, L., and D.P. Lesmes, 2002. Electrical-hydraulic relationships observed for
457 unconsolidated sediments. *Water Resources Research*, 38(10):1213.
458 doi:10.1029/2001WR001075.
459 Tabbagh, A., P. Cosenza, A. Ghorbani, R. Guérin, and N. Florsch, 2009. Modelling of
460 Maxwell–Wagner induced polarisation amplitude for clayey materials. *Journal of*
461 *Applied Geophysics*, 67(2):109‐13. doi:10.1016/j.jappgeo.2008.10.002.
462 Titov, K., A. Tarasov, Y. Ilyin, N. Seleznev, and A. Boyd. 2010. Relationships between
463 Induced Polarization Relaxation Time and Hydraulic Properties of Sandstone.
464 *Geophysical Journal International*, 180(3):1095‐1106. doi:10.1111/j.1365-
465 246X.2009.04465.x.
466 Vanhala, H., and H. Soininen, 1995. Laboratory Technique for Measurement of Spectral
467 Induced Polarization Response of Soil samples. *Geophysical Prospecting*, 43(5):
468 655‐76. doi:10.1111/j.1365-2478.1995.tb00273.x.
469 Vanhala, H., H. Soininen, and I. Kukkonen. 1992. Detecting organic chemical contaminants

by spectral-induced polarization method in glacial till environment . *Geophysics*, 57 (8): 1014‐17. doi:10.1190/1.1443312.

Vinegar, H., and M. Waxman. 1984. Induced polarization of shaly sands. *Geophysics*, 49 (8): 1267‐87. doi:10.1190/1.1441755.

Zimmermann E., Kemna A., Berwix J., Glaas W., Münch H. M and Huisman J. A., 2008. A High-Accuracy Impedance Spectrometer for Measuring Sediments with Low Polarizability. *Measurement Science and Technology*, 19(10):105603. doi:10.1088/0957-0233/19/10/105603.

Zonge, K.L., 1972. Electrical properties of rocks as applied to geophysical prospecting. http://arizona.openrepository.com/arizona/handle/10150/287835.